Building Tomorrow's Society
Bâtir la Société de Demain

Fredericton, Canada
June 13 – June 16, 2018/ *Juin 13 – Juin 16, 2018*

FLEXURAL BEHAVIOUR OF SHAPE MEMORY ALLOY REINFORCED CONCRETE BEAMS

Elbahy, Yamen I.[1,2], and Youssef, Maged A.[1]
[1] Western University, Canada
[2] yelbahy@uwo.ca

Abstract: Trend of using smart structures, that can adjust their behaviour when exposed to severe unexpected loading, is increasing. One of the methods to achieve such structures relies on smart materials. For example, replacing conventional steel reinforcing bars in Reinforced Concrete (RC) structures with superelastic Shape Memory Alloy (SMA) bars significantly reduces the residual deformations caused by post-yielding behaviour. This paper provides in-depth understanding of the flexural behaviour of SMA RC beams. A sectional analysis method, that predicts the flexural behaviour of SMA RC beams during both loading and unloading stages, is adopted and validated using available experimental data. An extensive parametric study is then carried out to investigate the effect of different geometrical properties. Recommendations for the optimum amount and length of SMA bars are drawn based on results of this study.

1 INTRODUCTION

Reinforced Concrete (RC) beams are designed to withstand reversed cyclic bending moments during earthquake events. These moments can cause permanent deformations and rotations, which complicate future retrofit efforts or make the structure irreparable.

Superelastic Shape Memory Alloys (SMAs) are set of smart alloys that can undergo large deformations and return to their undeformed shapes upon unloading. They also have exceptional behaviour under cyclic loads (i.e. flag shaped stress-strain). They can undergo large number of inelastic loading/unloading cycles, while keeping zero or very small residual deformations upon load removal (Alam et al. 2007). In addition, SMAs have exceptional resistance to corrosion and fatigue loads (Janke et al. 2005). These unique properties have highly motivated researchers to utilize SMAs in different engineering applications. Yet, the use of SMAs in the structural engineering field is considered relatively new.

The use of SMAs as primary reinforcing bars in RC structures is a high potential application. Up to now, this application is mainly covered in the research field with few real applications. For example, Saiidi et al. (2007) tested simply supported beams that have external SMA reinforcement in the mid-span region. Test results showed that the use of SMA bars led to significantly reduced residual deformations upon unloading as compared to conventional steel bars. Elbahy et al. (2009) conducted extensive analytical studies to develop design equations of SMA RC members. The developed equations serve both strength and serviceability requirements. In real applications, SMAs have been used in the rehabilitation of the S. Giorgio Church Bell-Tower in Italy (Indirli et al. 2001) and a RC bridge in Michigan. (Soroushian 2001).

The high cost of SMAs as compared to conventional steel bars and the large size of civil structures limit their use as primary reinforcement. To overcome this problem, researchers suggested limiting the length and position of SMA bars to critical regions of the structure (Youssef et al. 2008; Abdulridha et al. 2013).

This suggestion facilitates using SMA bars in real applications. However, there are no guidelines or standards to estimate the needed amount and length of the SMA reinforcement. Thus, the aim of this study is to develop such guidelines.

2 RESEARCH SIGNIFICANCE

RC structures are seismically designed to satisfy the strong column-weak beam concept, where the earthquake energy is dissipated in the form of steel yielding. Under moderate to strong earthquakes, severe permanent deformations are expected. These permanent deformations can make the structure irreparable. Thus, there is a need to minimize these permanent deformations. One way to do this is by using smart materials such as SMAs.

There are no guidelines or design tools that can be used to determine the optimum amount and length of SMA bars. This study aims at developing simple design equations that can be used by practitioners to design the SMA RC beams.

3 ANALYSIS METHOD

The flexural behaviour of steel and SMA RC cross-sections is analytically investigated in this paper. The analysis method is based on the sectional analysis approach, which uses fibre modelling (Youssef and Rahman 2007; Elbahy et al. 2009). The main idea lies in dividing the studied cross-section into discrete number of horizontal fibres. Utilizing the one-dimensional constitutive relationship of each fibre, and taking into account the cross-section equilibrium and kinematics, the mechanical behaviour of the cross-section is obtained.

A displacement-controlled loading technique is used in the analysis, where the cross-section is subjected to curvature values in an incremental way. During the unloading stage, the load is also incrementally removed. Two main assumptions are: (i) plane sections remain plane (i.e. linear strain distribution); and (ii) perfect bond exists between concrete and the reinforcement.

Four different materials models are implemented in the developed program. These models represent the behaviour of concrete, steel, and SMA under tensile and compressive loadings. Brief description of these models is introduced in the following subsections.

3.1 Concrete under compression

The model developed by Scott et al. (1982), Figure 1(a), is used to model the concrete behaviour under compression loading. This model represents a good balance between accuracy and simplicity. During the unloading stage, behaviour of concrete in compression is assumed to follow the model proposed by Karsan and Jirsa (1969). When unloading starts, the material follows linear straight path that connects the strain at the unloading start, ε_r, to the unloading strain at zero-stress, ε_p. After reaching ε_p, the strains continue to reduce while keeping the stress value equal to zero. This continues till reaching the point of zero strain.

3.2 Concrete under tension

Behaviour of concrete under tension loading is assumed to follow the model proposed by Stevens et al. (1987) and simplified by Youssef and Ghobarah (1999), Figure 1(b). In the pre-cracking zone, the concrete behaves in a linear fashion up to the cracking stress f_{cr}. This is followed by significant reduction in the stress value.

If unloading starts before reaching f_{cr}, the concrete behaves in a linear fashion similar to the loading stage. If unloading starts after reaching f_{cr}, the material follows a linear path with a slope equal to the modulus of elasticity of concrete. After reaching the zero-stress point, the strain continues to decrease while the stress is kept equal to zero. This continues until reaching the point of zero-strain.

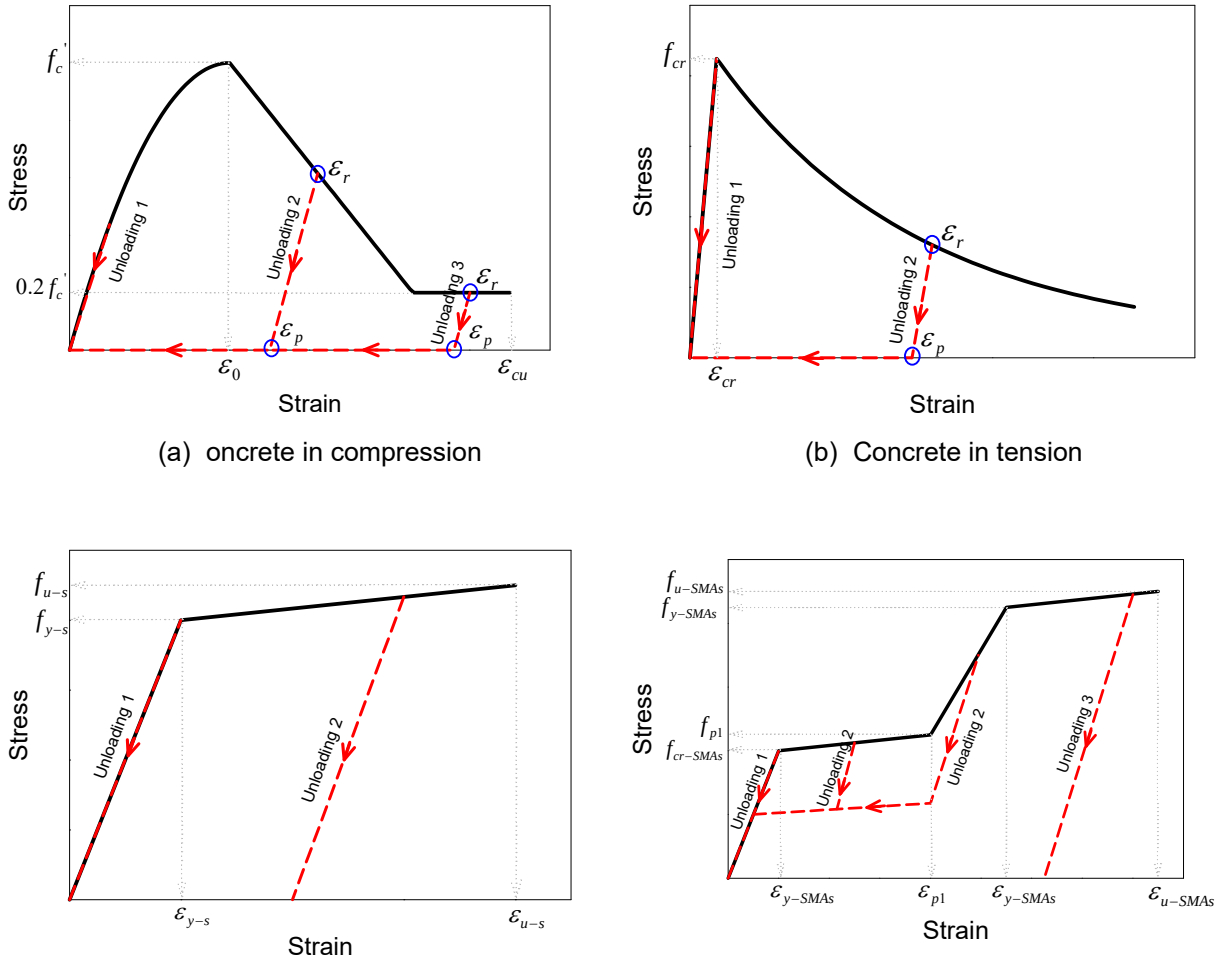

(a) oncrete in compression

(b) Concrete in tension

(c) Steel in tension/compression

(d) SMA in tension/compression

Figure 1: Stress-strain models during loading and unloading stages

3.3 Steel bars

The behaviour of the steel material is assumed to follow a bilinear stress-strain relationship under both tension and compression loadings, Figure 1(c). The material behaves elastically until reaching its yielding strain, $\varepsilon_{y\text{-}s}$. Then, the modulus of elasticity is significantly reduced.

If unloading starts within the pre-yielding zone, the material behaves in an elastic manner similar to the loading stage with no residual deformations at complete unloading. If the unloading starts within the post-yielding zone, the material follows a linear unloading path until yielding on the other side (tension or compression).

3.4 Superelastic SMA bars

The stress-strain model of SMA consists of four linear branches that are connected by smooth curves (Alam et al. 2007), Figure 1(d). To simplify the modelling process of the SMA material, the smooth curves are ignored and linear branches are assumed to directly intersect. The material behaves elastically until reaching the SMA critical stress $f_{cr\text{-}SMA}$ which represents the start of the martensite stress induced transformation. Exceeding this limit, the material stiffness significantly reduces to about 10% of its initial value. If loading continues until full transformation to martensite phase occurs, the material regains about

50% of its initial stiffness. If loading continues to the real yielding limit, another significant reduction in the material stiffness occurs.

The behaviour of SMAs during the unloading stage is illustrated in Figure 1(d). If unloading starts before reaching SMAs critical stress, the material behaves in an elastic manner similar to the loading stage (i.e. unloading path 1). If unloading starts when the stress in the material is in between the critical and yielding stresses, the material follows a flag shaped stress-strain relationship (i.e. unloading path 2). If unloading starts after the material reaches its yielding limit), the material follows a linear unloading path (i.e. unloading path 3).

4 EXPERIMENTAL VALIDATION

The experimental work performed by Abdulridha (2013) and Abdulridha et al. (2013) is used to validate the developed model. Six simply supported beams with dimensions of 2800 mm length, 2400 mm span, 125 mm cross-section width, 250 mm cross-section height, and reinforced with SMA and/or steel bars are experimentally tested. All beams are tested under two central point loads spaced at 125 mm around mid-span.

The clear concrete cover of the beams is 20 mm. The average concrete compressive strength is 32.7 MPa for the SMA RC beams and 34.6 MPa for the steel RC beam. The beams are transversely reinforced with 6.35 mm wires spaced at 100 mm.

The length of the SMA bars is 600 mm centred at the mid-span of the beams. The diameter of the middle 300 mm of the SMA bars is reduced to 9.50 mm. M15 steel bars connected the SMA bar using mechanical couplers are used to reinforce the remaining length of the beam. Reinforcement details of the tested beams are summarized in Table 1.

The developed program is used to perform moment-curvature analysis of the different cross-sections of the studied beams. The moment-curvature diagrams for three different cross-sections of B6-NR are shown in Figure 2: (i) 2-9.5mm SMA RC cross-section; (ii) 2-12.7 mm SMA RC cross-section; and (iii) 2-15M steel RC cross-section. The moment-curvature analysis of each cross-section is performed up to the experimental unloading moment. Experimental load-displacement results are plotted versus the analytically obtained results for all beams in Figure 3. Very good agreement between the experimental and analytical results is obtained for all beams.

5 PARAMETRIC STUDY

A parametric study is carried out to investigate the effect of different geometrical and cross-sectional parameters on the overall behaviour of SMA RC beams during loading/unloading stages. Studied parameters include: (i) cross-section reinforcement ratio (ρ_{SMAs}); (ii) ratio between the amount of SMA reinforcement to the amount of steel reinforcement (A_{SMAs}/A_s); (iii) cross-section height-to-width ratio (h/b); (iv) beam span-to-depth ratio (L/h); and (v) concrete compressive strength (f_c).

The parametric study is performed on cantilever beams. The beams are reinforced with SMA bars at the fixed end of the beams and regular steel bars elsewhere. For each of the studied parameters, nine different lengths are considered for the SMA bars. The considered lengths are: $L/20$, $L/10$, $L/8$, $L/6$, $L/4$, $L/3$, $L/2$, and $L/1$, where L is the full length of the studied beam. The beams are loaded with single point loads applied at their free ends.

For each of the studied beams, the developed program is used to obtain the moment-curvature relationships of its cross-sections. The moment-area method is then used to obtain the load-displacement relationship. Results are then assessed based on: (i) load-displacement relationship; (ii) amount of residual deformations; (iii) change in flexural stiffness; and (iv) amount of dissipated energy.

Table 1: Details of the tested beams by Abdulridha et al. (2013).

Specimen	Loading type	Reinforcement type at mid-span	Longitudinal reinforcement at mid-span	
			Bottom	Top
B1-SM	Monotonic	Steel	2 bars, 10M	2 bars, ϕ = 6.35 mm
B2-SC	Cyclic	Steel	2 bars, 10M	2 bars, ϕ = 6.35 mm
B3-SR	Cyclic	Steel	2 bars, 10M	2 bars, 10M
B4-NM	Monotonic	SMAs	2 bars, ϕ = 9.5 mm	2 bars, ϕ = 6.35 mm
B6-NR	Cyclic	SMAs	2 bars, ϕ = 9.5 mm	2 bars, ϕ = 9.5 mm
B7-NCM	Cyclic	SMAs	2 bars, ϕ = 9.5 mm	2 bars, ϕ = 9.5 mm

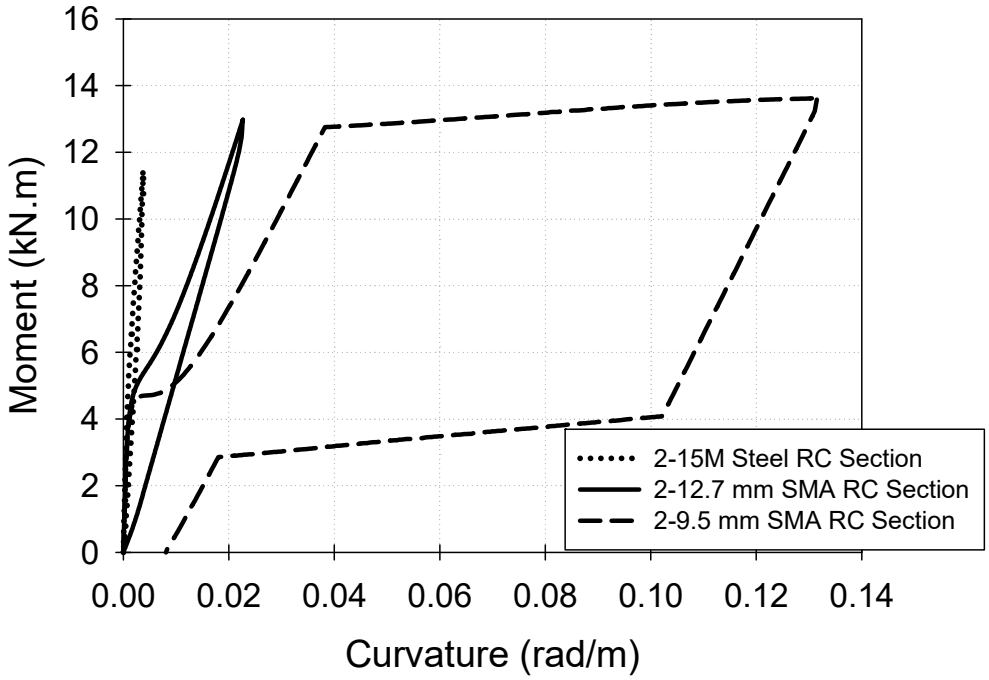

Figure 2: Moment-curvature analysis for steel and SMAs RC cross-sections.

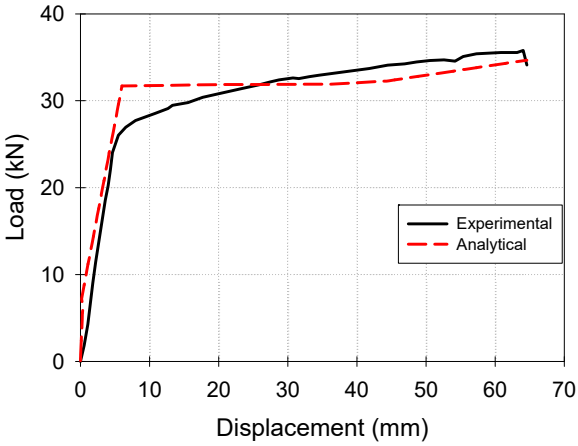

(a) B1-SM

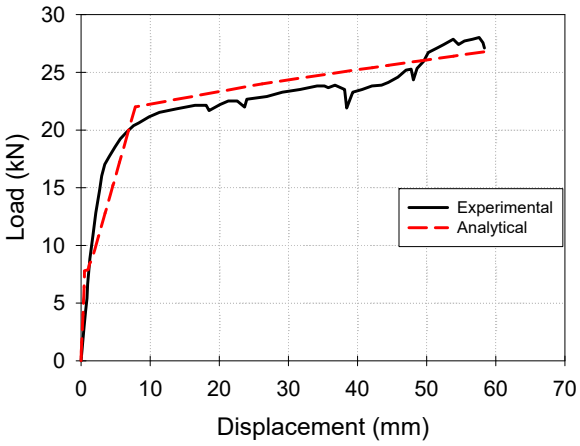

(b) B4-NM

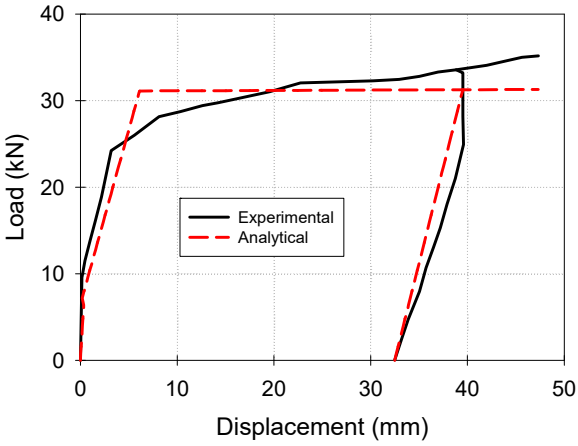

(c) B2-SC

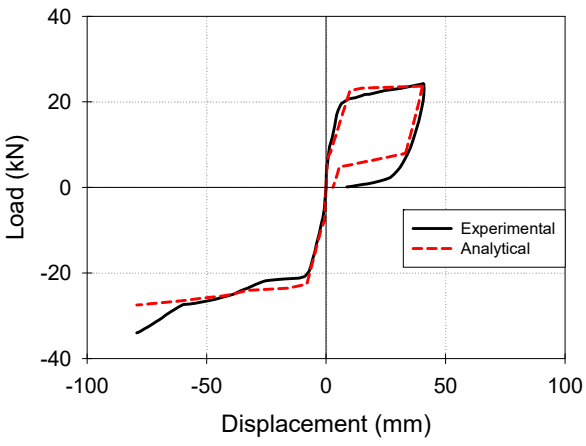

(d) B7-NC

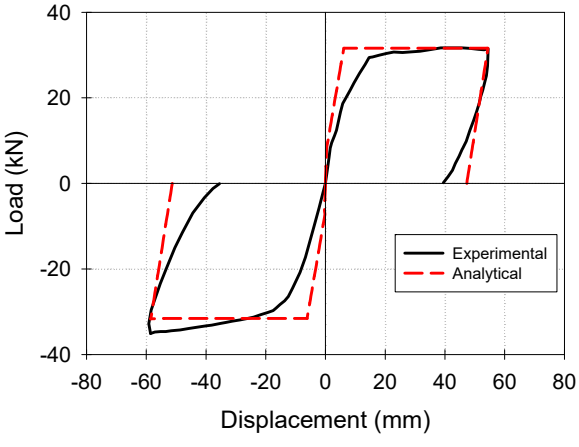

(e) B3-SR

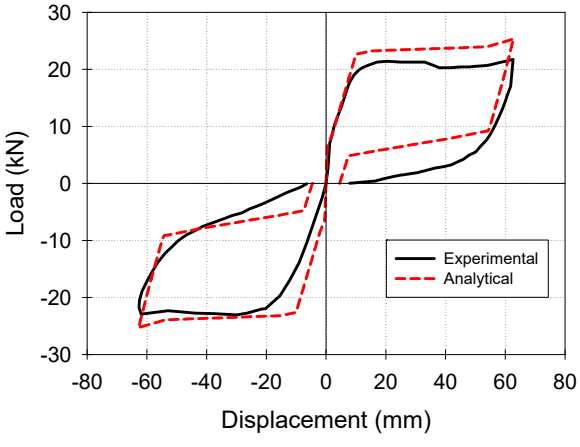

(f) B6-NR

Figure 3: Experimental vs. Analytical load-displacement relationships

6 CHOICE OF SMA LENGTH

There are only few real applications that utilized SMA bars as primary reinforcing bars. This section provides equations that can predict the residual displacements at complete unloading, the change in the beam stiffness, and the dissipated energy when regular steel bars are replaced with SMA bars. Multiple linear regression technique is used to determine these equations. Linear, quadratic power and logarithmic models are examined.

The database used in the analysis is created from the results obtained from the parametric study. The inputs used in the analysis are: L_{SMAs}/L, A_{SMAs}/A_s, $\rho_{SMAs}/\rho_{s\text{-}min}$, $\rho_{SMAs}/\rho_{s\text{-}b}$, f'_c, h/b, LL, L/h. The outputs used in the analysis are: δ_r/δ_{max}, $(\delta_{y\text{-}s}/\delta_{cr\text{-}SMAs})$, EN_{SMAs}/EN. The analysis starts with investigating the correlation between each pair of the variables. Correlation matrix is determined and is shown in Table 2.

As an example, Table 3 presents a linear regression model of δ_r/δ_{max} when $L_{SMAs}/L \leq 0.14$. The model defines the linear relationship between the dependent variable δ_r/δ_{max} and the second order transformation of the three independent variables (L_{SMAs}/L, A_{SMAs}/A_s, and L/h). The coefficient for each independent variable is estimated. All the variable coefficients are statistically significant from zero at 95% confidence level because the associated p-values of all the coefficients are less than 0.05. Measures of model goodness-of-fit (represented by *R-squared*, *Adj R-squared,* and *Root Mean Square Error (MSE)*) are also reported in the table. The model is considered to be with very good fit as its *R-squared* value is 0.9. Furthermore, the values of root MSE range is 0.10 confirming also a very good model fit

The final suggested regression models are summarized in Equations [1] to [3]:

[1a] $\delta_r/\delta_{max} = -9.38644 \times (L_{SMAs}/L) + 35.56246 \times (L_{SMAs}/L)^2 + 0.6020821 \times (A_{SMAs}/A_s) - 0.0932349 \times (A_{SMAs}/A_s)^2 - 0.1102018 \times (L/h) + 0.0085443 \times (L/h)^2 + 0.5670711 \quad L_{SMAs}/L \leq 0.14$

[1b] $\ln(\delta_r/\delta_{max}) = -0.9008659 \times (L_{SMAs}/L) + 1.213188 \times (A_{SMAs}/A_s) - 0.4609012 \times (L/h) + 0.0353669 \times (L/h)^2 - 1.027448 \quad L_{SMAs}/L > 0.14$

[2a] $\ln(\delta_{y\text{-}s}/\delta_{cr\text{-}SMAs}) = -2.871903 \times (L_{SMAs}/L) + 0.3076423 \times (A_{SMAs}/A_s) - 0.0438487 \times (A_{SMAs}/A_s)^2 - 0.0896358 \times (L/h) + 0.0066686 \times (L/h)^2 - 0.0422848 \quad L_{SMAs}/L \leq 0.14$

[2b] $\ln(\delta_{y\text{-}s}/\delta_{cr\text{-}SMAs}) = -0.2967487 \times (L_{SMAs}/L)^2 + 0.3830598 \times (A_{SMAs}/A_s) - 0.7221479 \times (\rho_{SMAs}/\rho_{s\text{-}b}) + 0.4479831 \times (\rho_{SMAs}/\rho_{s\text{-}b})^2 - 0.6942598 \quad L_{SMAs}/L > 0.14$

[3a] $EN_{SMAs}/EN_s = -4.246152x \times (L_{SMAs}/L) + 10.20425 \times (L_{SMAs}/L)^2 + 0.0130695 \times (A_{SMAs}/A_s)^2 + 0.9730266 \quad L_{SMAs}/L \leq 0.14$

[3b] $EN_{SMAs}/EN_s = -0.8652805x \times (L_{SMAs}/L) + 0.4895451x \times (L_{SMAs}/L)^2 + 0.0141995 \times (A_{SMAs}/A_s)^2 + 0.057189 \times (\rho_{SMAs}/\rho_{s\text{-}b}) + 0.6334503 \quad L_{SMAs}/L > 0.14$

Table 2: Correlation coefficients between all variables

	δ_r/δ_{max}	$\delta_{y\text{-}s}/\delta_{cr\text{-}SMAs}$	EN_{SMAs}/EN_s	L_{SMAs}/L	A_{SMAs}/A_s	$\rho_{SMAs}/\rho_{s\text{-}min}$	$\rho_{SMAs}/\rho_{s\text{-}b}$	f'_c	h/b	LL	L/h
δ_r/δ_{max}	1.00										
$\delta_{y\text{-}s}/\delta_{cr\text{-}SMAs}$	0.79	1.00									
EN_{SMAs}/EN_s	0.83	0.60	1.00								
L_{SMAs}/L	-0.46	-0.38	-0.76	1.00							
A_{SMAs}/A_s	0.51	0.70	0.23	0.00	1.00						
$\rho_{SMAs}/\rho_{s\text{-}min}$	0.10	0.09	0.10	0.00	0.27	1.00					
$\rho_{SMAs}/\rho_{s\text{-}b}$	0.07	0.04	0.08	0.00	0.21	0.97	1.00				
f'_c	0.16	0.25	0.06	0.00	0.26	-0.18	-0.32	1.0			
h/b	0.05	0.04	0.02	0.00	0.02	-0.02	-0.02	-0.3	1.0		
LL	0.32	0.42	0.08	0.00	0.47	0.00	-0.08	0.1	0.5	1.0	
L/h	-0.21	-0.32	-0.06	0.00	-0.30	0.09	0.17	-0.4	0.1	-0.4	1.0

Table 5: Regression model for δ_r/δ_{max} when $L_{SMAs}/L \leq 0.14$

Source	SS	df	MS			
Model	5.40512271	6	0.900853784	Number of obs	=	64
				F(6, 57)	=	86.64
				Prob > F	=	0
Residual	0.592698607	57	0.010398221	R-squared	=	0.9012
				Adj R-squared	=	0.8908
Total	5.99782131	63	0.095203513	Root MSE	=	0.10197

δ_r/δ_{max}	Coef.	Std. Err.	t	P>t	[95% Conf.	Interval]
L_{SMAs}/L	-9.38644	1.010386	-9.29	0	-11.4097	-7.363177
$(L_{SMAs}/L)^2$	35.56246	7.852247	4.53	0	19.83861	51.28632
A_{SMAs}/A_s	0.6020821	0.0976462	6.17	0	0.406549	0.7976151
$(A_{SMAs}/A_s)^2$	-0.0932349	0.0205793	-4.53	0	-0.1344443	-0.0520255
L/h	-0.1102018	0.0431388	-2.55	0.013	-0.1965858	-0.0238178
$(L/h)^2$	0.0085443	0.0038105	2.24	0.029	0.0009139	0.0161747
Constant	0.5670711	0.1381184	4.11	0	0.2904937	0.8436485

7 CONCLUSIONS

In this study, flexural behaviour of SMA RC beams during loading/unloading stages is investigated. Analysis method, that is based on the sectional analysis approach, is used to investigate the flexural behaviour of steel and SMA RC beams. First, the applicability of using the moment-area method with SMA RC beams is validated using available experimental results.

An extensive parametric study is then carried out to investigate the effect of different geometrical and cross-sectional parameters on the flexural behaviour of SMA RC beams. Studied parameters are: (i) cross-section reinforcement ratio; (ii) ratio between the amounts of SMA reinforcement to the amount of steel

reinforcement; (iii) cross-section height-to-width ratio; (iv) beam span-to-depth ratio; and (v) concrete compressive strength. For each of the studied parameters, nine load-displacement responses are calculated assuming different lengths of the SMA bars.

Results of the parametric study are then used for multiple linear regression analysis. Results of the regression analysis are used to develop equations to help designers address the change occurring in the beam behaviour when regular steel reinforcing bars are replaced with SMA reinforcing bars. Changes in the amounts of residual displacements, flexural stiffness and dissipated energy can be estimated using the developed equations.

8 REFERENCES

Abdulridha, A. 2013. Performance of Superelastic Shape Memory Alloy Reinforced Concrete Elements Subjected to Monotonic and Cyclic Loading. PhD Thesis, Department of Civil Engineering, University of Ottawa, Ottawa, Ontario, Canada, 346 pp.

Abdulridha, A., Palermo, D., Foo, S., and Vecchio, F. J. 2013. Behavior and Modeling of Superelastic Shape Memory Alloys Reinforced Concrete Beams. Journal of Engineering Structures, 49, 893-904. DOI: 10.1016/j.engstruct.2012.12.041.

Alam, M.S., Youssef, M.A., and Nehdi, M. 2007. Utilizing Shape Memory Alloys to Enhance the Performance and Safety of Civil Infrastructure: a Review." Canadian Journal of Civil Engineering, **34**(9), 1075-1086.

Elbahy Y.I., Youssef M.A., Nehdi M. 2009. Stress Block Parameters for Concrete Flexural Members Reinforced with Superelastic Shape Memory Alloys. Journal of Materials and Structures, **42**(10), 1335-1351.

Janke, L., Czaderski, C., Motavalli, M., and Ruth, J. 2005. Applications of Shape Memory Alloys in Civil Engineering Structures - Overview, Limits and New Ideas. Materials and Structures, **338**(279), 578-592.

Karsan, I. D., and Jirsa, J. O. 1969. Behavior of Concrete under Compressive Loading. ASCE Journal (Structural Division), **95**(12), 2543-2563.

Scott, B.D.; Park, R.; and Priestley, M.J.N. 1982. Stress-Strain Behavior of Concrete Confined by Overlapping Hoops at Low and High Strain Rates. ACI journal, **79**(1), 13-27.

Stevens, N.J., Uzumeri, S.M., and Collins, M.P. 1987. Analytical Modeling of Reinforced Concrete Subjected to Monotonic and Reversed Loading. Publication No. 87-1, University of Toronto, 3634 p.

Youssef, M., and Ghobarah, A. 1999. Strength Deterioration due to Bond Slip and Concrete Crushing in Modeling of Reinforced Concrete Members. ACI Structural Journal, **96**(6), 956-967.

Youssef, M.A., and Rahman, M. 2007. Simplified seismic modeling of reinforced concrete flexural members. Magazine of Concrete Research, **59**(9), 639-649.